

## Synthesis and Structural Investigations of Cu, Mn doped $Cd_{1-x}Zn_xS$ Quantum Dots

INDU YADAV<sup>a</sup>, DHARAMVIR SINGH AHLAWAT<sup>a\*</sup>, RACHNA AHLAWAT<sup>a</sup>

<sup>a</sup>.Department of Physics, Chaudhary Devi Lal University, Sirsa-125055 (Hry.), India

\*Corresponding Author E-Mail: dahlawat66@gmail.com

Received: 12.03.2018

Accepted: 23.04.2018

Published Online 15.06.2018

<https://doi.org/10.30731/ijcps.7.3.2018.1-9>

### Abstract

A desirable quality of copper and manganese codoped  $Cd_{1-x}Zn_xS$  ( $x \leq 1$ ) quantum dots have been synthesized successfully using chemical co-precipitation method at room temperature. Structural investigations of the synthesized samples were carried out by powder XRD, TEM FTIR and AFM techniques. Further, the XRD results confirm that Cu and Mn codoped  $Cd_{1-x}Zn_xS$  nanocrystallites exhibit wurtzite structure. Lattice strain and average nanocrystallite size in the range 2-4 nm have been determined. The FTIR analysis identifies absorption peaks of Cd-S/Zn-S stretching modes along with presence of some moisture content in the synthesized samples. The TEM analysis further confirms polycrystalline nature of Cu, Mn doped  $Cd_{1-x}Zn_xS$  ( $x \leq 1$ ) nanocrystallites by SAED pattern and corresponding histograms give the particle size distribution.

**Keywords:** Co-precipitation;  $Cd_{1-x}Zn_xS$ :(Cu,Mn) nanocrystallites; XRD; FTIR; TEM; AFM.

### Introduction

Band structures, electronic and optical properties of semiconductors which are based on Cd, Zn and Hg in combination with sulphur, selenium and tellurium have been reported by many investigators by theoretical methods.<sup>1</sup> In this direction, synthesis of ternary metal chalcogenides of group II-VI semiconductors in nanocrystalline form has become a rapidly growing area of research due to their important luminescent properties, quantum confinement effects and other important physical and chemical properties.<sup>2</sup> From the last decade, the wide band gap nanocrystalline materials like CdS, ZnS, CdSe, ZnSe have been investigated by many researchers<sup>3-5</sup> but research work on their doped ternary alloy nanostructures is found still in a limited way. Although, the band gap of binary semiconducting materials can be tuned by changing the particle size while in the case of ternary semiconducting materials it can also be tuned by changing the percentage of composition of its constituents.<sup>4</sup> In these materials like cadmium chalcogenides, it is possible to engineer the band gap over a wide range depending upon the concentration of Cd and Zn in the CdZnS system that opens a new avenue for tremendous potential applications in diverse areas like solar cells, photo-catalysis, sensors, photonic, and other optoelectronic devices.<sup>5,6</sup> Recently, cadmium zinc sulfide (CdZnS) ternary compounds are being widely used as wide band gap window materials in heterojunction solar cells and photoconductive devices. Interestingly, in solar cell systems, CdS films have been demonstrated to effectively replace by the higher band gap ternary material such as a CdZnS compound that leads to a decrease in window absorption loss. Eventually, an increase in the short-circuit current in the solar cell has been reported.<sup>7</sup> Thus CdZnS

ternary compounds are potentially useful as window materials for the fabrication of p-n junctions without the lattice mismatch in the devices based on quaternary materials. The potentiality of such types of nanocrystals can further be exploited by doping with optically active luminescent centers to create new opportunities for other important applications in optoelectronics devices.

Because of their unique optical properties, discrete energy states can be introduced within the band gap of these ternary type semiconductors by doping with suitable transition metals such as Cu, Ag and Mn etc<sup>8</sup>. In the present course of work study, the dopants like Cu and Mn have been selected as dopants to serve two purposes; one as a luminescence activator and other as a compensator of n type materials for the II-VI group semiconductors.<sup>9</sup> However, presence of two different kinds of ions simultaneously in a host material produce fluorescence which is completely different from the emission due to a single doped ion and this property has been found very beneficial for white light generation.<sup>10</sup> Although, a lot of work on co-doping in binary semiconductors has been reported by many workers<sup>11,12</sup> and only a few investigation exist in the case single ion doping in CdZnS.<sup>8,13</sup> But the work of co-doping in the case of ternary semiconducting nanomaterials CdZnS is found very rare. These types of optical materials have been widely used in photonics and by doping with different transition metals; we can significantly improve their optical properties to a large extent. In light of the above mentioned importance, we have successfully synthesized Cd<sub>1-x</sub>Zn<sub>x</sub>S: Cu, Mn (x<1) ternary codoped alloy by using co-precipitation method and investigated their structural properties by powder XRD, FTIR and TEM.

## Experimental details

### Chemicals used

Cadmium acetate dihydrate (Cd(CH<sub>3</sub>COO)<sub>2</sub>·2H<sub>2</sub>O), Triethylamine (N(CH<sub>2</sub>CH<sub>3</sub>)<sub>3</sub>), copper acetate monohydrate (Cu(CH<sub>3</sub>COO)<sub>2</sub>·H<sub>2</sub>O), manganese acetate tetrahydrate (Mn(CH<sub>3</sub>COO)<sub>2</sub>·4H<sub>2</sub>O) and urea (NH<sub>2</sub>CONH<sub>2</sub>) were purchased from Sigma Aldrich. Zinc acetate dihydrate (Zn (CH<sub>3</sub>COO)<sub>2</sub>·2H<sub>2</sub>O) and thiourea (NH<sub>2</sub>CSNH<sub>2</sub>) have been used as the source material for Zn and S ions and purchased from the Loba Chemie.

### Precursors used

In this work, all chemicals were used as such without further purification. Furthermore, double distilled water was used as a solvent for all chemical reactions. We are using acetate as a precursor group. About 0.5 M cadmium acetate and zinc acetate were taken according to their molar ratio in a beaker known as Ist beaker and add 100 ml double distilled water and stirred about half an hour at a temperature 60°C. In an another beaker or conical flask (500ml) 1M urea, 1M thiourea were taken, dissolved in 100 ml of double distilled water and stir it for half an hour under normal stirring rate 450 rpm.

### Synthesis of Cu, Mn doped Cd<sub>1-x</sub>Zn<sub>x</sub>S (0 ≤ x ≤ 1) quantum dots

In the first beaker 0.01M of copper acetate monohydrate and manganese acetate tetrahydrate as dopants were added. The solution of first beaker was added drop wise in the second beaker under vigorous stirring at a temperature 60°C. As a result of this the color of the solution changes light yellow to deep yellow during the reaction. After completion of stirring the precipitates were left undisturbed for one day and then washed and filtered. Then the precipitates were dried in an air oven at a temperature 90°C for 8 hours. Finally, they were crushed in powder form using a pestle mortar and used for their characterization. Following the same procedure, six different samples were synthesized and coded their

names as S1, S2, S3, S4, S5 and S6 corresponding to the material composition CdS:Cu,Mn; Cd<sub>0.9</sub>Zn<sub>0.1</sub>S:Cu,Mn; Cd<sub>0.7</sub>Zn<sub>0.3</sub>S:Cu,Mn; Cd<sub>0.5</sub>Zn<sub>0.5</sub>S:Cu,Mn; Cd<sub>0.3</sub>Zn<sub>0.7</sub>S:Cu,Mn and Cd<sub>0.1</sub>Zn<sub>0.9</sub>S:Cu,Mn, respectively. However the dopants concentration Cu (0.01M) and Mn (0.01) was kept fixed for synthesis of all the samples. In this case we also observe that the color of precipitates at particular concentration of zinc changes as observed in case of single (Cu) doped series of CdZnS. The yellowness of the precipitates decreases as we increase the concentration of zinc and at x=1 we obtained white color precipitates, which confirms the formations of ZnS. This nomenclature of samples has been used throughout the paper to avoid complexity.

### Characterization

The X-ray diffraction (XRD) patterns of the powdered samples were recorded on a XRD X'Pert PRO with CuK $\alpha$  ( $\lambda=0.15406$  nm) radiation at an operating voltage 45 kV and operating current at 40 mA with a scanning rate 2 degree min<sup>-1</sup> from  $2\theta = 20^\circ$  to  $60^\circ$ . A SHIMADZU IR Affinity-1 FTIR spectrometer was used in the range 400-4000 cm<sup>-1</sup> for identification of different functional groups present in the precursors. For FTIR studies, the samples were mixed homogeneously with KBr and pellets of the desired dimensions were prepared. Morphology of the synthesized samples was also observed on a FEI TECNAI G<sup>2</sup> high resolution transmission electron microscope (HRTEM) operated at 200 kV. Different samples were prepared for TEM measurements by dispersed in ethanol and then kept in a sonicator up to five minutes. After that the solution was dripped onto a carbon coated copper grid and dried at room temperature.

## Results and discussion

### XRD analysis

Fig. 1(a) shows X-ray diffraction (XRD) patterns of Cu and Mn doped Cd<sub>1-x</sub>Zn<sub>x</sub>S (x<1) nanocrystalline samples. The XRD of sample S1 exhibits diffraction peaks at different values of  $2\theta \sim 25.10^\circ, 26.82^\circ, 28.18^\circ, 43.96^\circ, 48.24^\circ$  and  $52.37^\circ$  corresponding to the (100), (002), (101), (110), (103) and (112) reflection planes, respectively. The crystal structure of sample S1 is well matched with wurtzite form (JCPDS data file no.01-0783) having preferential orientation along (002) plane.<sup>14</sup> Further, with the increase of Zn content (x=0.3) in the sample S3, two small peaks have been appeared at  $2\theta \sim 28.32^\circ$  and  $39.72^\circ$  corresponding to (101) & (102) planes of hexagonal structure.<sup>15</sup> Also, the existing diffraction peaks become broader as compared to sample S1 due to quantum size effect.

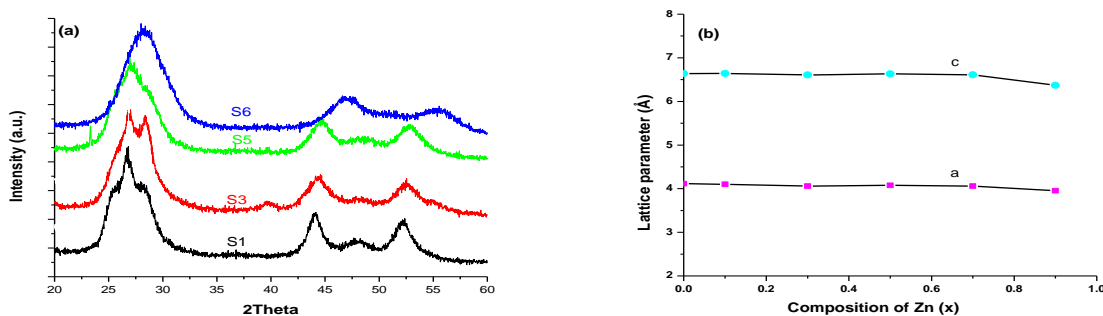


**Fig.1 (a)** XRD pattern and **(b)** Variation of lattice parameters of Cd<sub>1-x</sub>Zn<sub>x</sub>S: Cu, Mn ternary alloy at different values of mole fraction (x).

Further, no characteristic peaks of the doping impurities Cu, Mn are observed in the XRD pattern. It is also noticed that the diffraction peaks have shifted slightly towards the higher angle when the Zn concentration increases which confirm the formation of the homogenous alloy of CdZnS<sup>16</sup>. However, T. T. Nguyen et al<sup>17</sup> observed phase transition from zinc blende to wurtzite in Cu, Al doped ZnS at much higher temperature ~ 450-500°C. From XRD data, the d-value for all prepared samples has been calculated using the well-known Bragg's relation whose results are given in table 1. The crystallite size has been calculated using Debye Scherrer's<sup>14</sup> formula as given below, where the symbols have their usual meanings:

$$D = k \lambda / \beta \cos \theta \quad (1)$$

The experimental values of lattice constants 'a' and 'c' for hexagonal phase of CdZnS alloy were also calculated by using the relation (2) as given in the table 1:

$$1/d^2 = 4/3.(h^2 + hk + k^2)/ a^2 + l^2/c^2 \quad (2)$$

**Table 1:** Structural parameters based on XRD data for the samples.

Sample code	Peak Position (2θ)	Particle size D <sub>D-S</sub> (nm)	a(Å)	c(Å)	d (Å)	Volume of unit cell (Å) <sup>3</sup>	Lorentz Factor (L)
S1	26.62	2.44	4.113	6.637	3.319	97.27	4.786
S2	26.62	2.16	4.100	6.641	3.321	96.68	4.784
S3	26.98	2.16	4.060	6.607	3.304	94.35	4.759
S4	26.92	2.29	4.076	6.631	3.316	95.41	4.777
S5	27.02	2.04	4.057	6.612	3.306	94.28	4.741
S6	27.79	2.04	3.951	6.369	3.185	86.14	4.411

**Note:** S1=CdS:Cu,Mn; S2=Cd<sub>0.9</sub>Zn<sub>0.1</sub>S:Cu,Mn; S3=Cd<sub>0.7</sub>Zn<sub>0.3</sub>S:Cu,Mn; S4=Cd<sub>0.5</sub>Zn<sub>0.5</sub>S:Cu,Mn; S5=Cd<sub>0.3</sub>Zn<sub>0.7</sub>S:Cu,Mn and S6=Cd<sub>0.1</sub>Zn<sub>0.9</sub>S:Cu,Mn

The volume of the unit cell for hexagonal system has been calculated using the following equation (3) as given below.

$$V = \sqrt{3/2}.a^2c \quad (3)$$

In the Fig. 1(b), variation of lattice parameters with Zn (x) composition has been graphically demonstrated. It was observed from Fig. 1(b) that there is a slightly decrease in lattice parameters as we increase the Zn content whose values are given in the table 1. The most probable reason for such a behavior of the nanomaterial is understood due to the smaller atomic radii of Zn<sup>2+</sup> ion (0.74 Å) as compared to the Cd<sup>2+</sup> ion (0.97 Å) and Zn<sup>2+</sup> ion replace the Cd<sup>2+</sup> ion, therefore lattice is contracted<sup>18,19</sup>. Furthermore, the Lorentz factor has also been calculated which depends on the Bragg angle/diffraction

geometry and gives the distribution of diffraction planes in the powder samples. The diffraction from nanoparticles is oriented randomly in the powder specimen at or near the Bragg angle of a given (hkl) plane gives the different diffraction intensity<sup>14</sup>. Lorentz factor for the samples under study was calculated from the given relation (4).

$$L=1/4\sin^2\theta\cos\theta \quad (4)$$

We can determine the crystallite size and lattice strain present in the sample by using Williamson-Hall relation<sup>20</sup> which is given by equation (5).

$$\beta_{hkl} \cos\theta = K\lambda/D_{W-H} + 4\epsilon \sin\theta \quad (5)$$

where  $\lambda$  is the wavelength of X- ray used,  $K= 0.9$  for uniform small size crystals,  $\theta$  is the Bragg diffraction angle,  $\epsilon$  is the strain and  $D_{W-H}$  is the average crystallite size by W-H method. A graph is plotted between  $\beta \cos\theta$  versus  $\sin\theta$  of the each peak and their linear fit gives the slope from which strain  $\epsilon$  is calculated and the crystallite size is estimated from the intercept on y-axis. The  $\beta$  was calculated from the each peak at full width at half maximum (FWHM). The XRD peak broadening due to the small crystallite size and lattice strain present in the material, can be distinguished from W-H plot as shown in Fig 2.

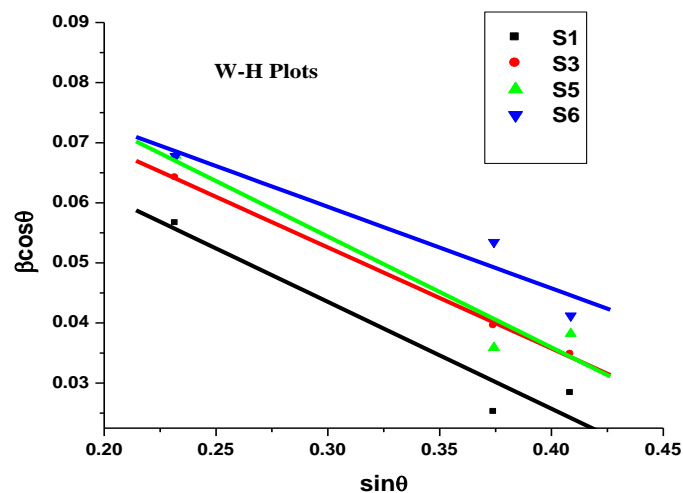


**Fig. 2:** W- H plot of  $Cd_{1-x}Zn_xS:Cu, Mn$  alloy at different values of mole fraction ( $x=0, 0.3, 0.7, 0.9$ ).

It has been observed from the W-H plot that the crystallite size decreases which may be due to the negative strain present in the sample<sup>17</sup> as shown in table 2. This negative strain is induced in the sample by the substitution of  $Cd^{2+}$  ( $0.97 \text{ \AA}$ ) ion by the  $Zn^{2+}$  ( $0.74 \text{ \AA}$ ) ion in the  $CdZnS$  lattice which compress the lattice due to lower ionic radii of  $Zn^{2+}$  ion. Moreover, Deshpande et. al.<sup>21</sup> have also been reported the negative strain in the  $ZnSe$  nanocrystallites which mainly due to the compressive strain of  $ZnSe$  nanomaterials.

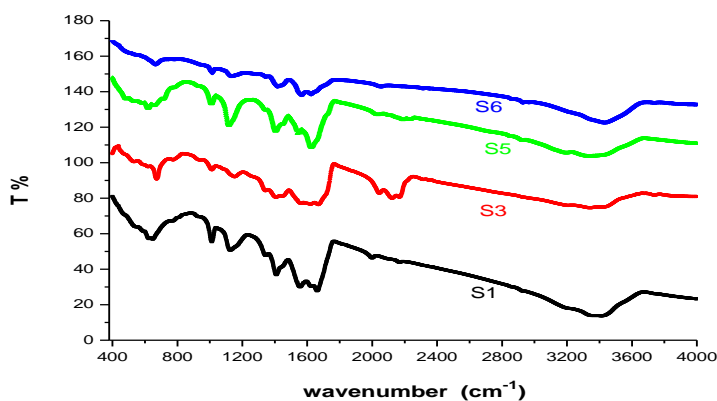
**Table 2:** Size and strain of the prepared samples using W-H plots.

Sample	$D_{W-H}$ (nm)	$D_{TEM}$ (nm)	Strain $\epsilon$	Dislocation density $1/\langle D \rangle^2$ ( $\rho$ )
S1	1.43	4	-0.0444	0.167
S3	1.42	3.5	-0.03619	0.214
S5	1.36	3	-0.03829	0.240
S6	1.43	2.5	-0.02866	0.240

The overall calculated data of XRD analysis and the phase transition at room temperature in Cu, Mn codoped CdZnS ternary alloy indicated the potential advantages of these materials for glass based optoelectronic device fabrications<sup>7</sup>.

#### Fourier transform infrared spectroscopy (FTIR)

Fig. 3 shows the FTIR spectra of Cu, Mn doped  $Cd_{1-x}Zn_xS$  samples ( $x=0, 0.3, 0.7, 0.9$ ) in the range  $400-4000\text{ cm}^{-1}$ . The different functional groups are identified due to absorption of IR radiation in a specific wave number by each group. In the higher energy regions, a peak of O-H stretching of absorbed water molecules has been appeared at  $3410-3360\text{ cm}^{-1}$ . The strong absorption centered at  $1012, 1126, 1409$  and  $1660\text{ cm}^{-1}$  are due to the symmetric stretching of acetate  $COO^-$  group of initial precursors<sup>15</sup>.


**Fig. 3:** FTIR spectra of  $Cd_{1-x}Zn_xS$ : Cu, Mn ternary alloy at different values of mole fraction.

However in sample S3 IR absorption peaks occur at  $2167, 2123$  and  $2044\text{ cm}^{-1}$  which may be due to some microstructural deformation present in the sample. In literature, these peaks are corresponds to  $C-N/C=S$  of thiourea and isothiocyanate ( $-NCS$ ) which formed due to hydrolysis of thiourea during the synthesis<sup>22</sup>. However, in lower energy region a small peak at  $661\text{ cm}^{-1}$  has been assigned to Cd-S/Zn-S stretching mode<sup>22</sup> and its absorption decreased as the concentration of Zn increases in the samples. In the present study, the information is detected from the samples due to the interaction of IR light with matter through the physical processes of stretching, contraction and bending of chemical bonds of the functional groups. The existence of respective absorption peaks and bands in FTIR spectrum confirms the formation

of CdZnS with the impurities traces (because of chemical reaction of different precursors used), and water molecules or hydroxide ions in the prepared nanocrystallites.

### TEM analysis

Transmission Electron Microscopy was used to study morphology of the samples which gives the size, shape and nano crystalline nature. Fig. 4 shows the TEM micrographs of Cu, Mn doped  $Cd_{1-x}Zn_xS$  ( $x = 0.0, 0.3, 0.7, 0.9$ ) namely S1, S3, S5 and S6 samples. In this study the smallest and largest nanocrystallite sizes were found about 2.0 and 4 nm, respectively.

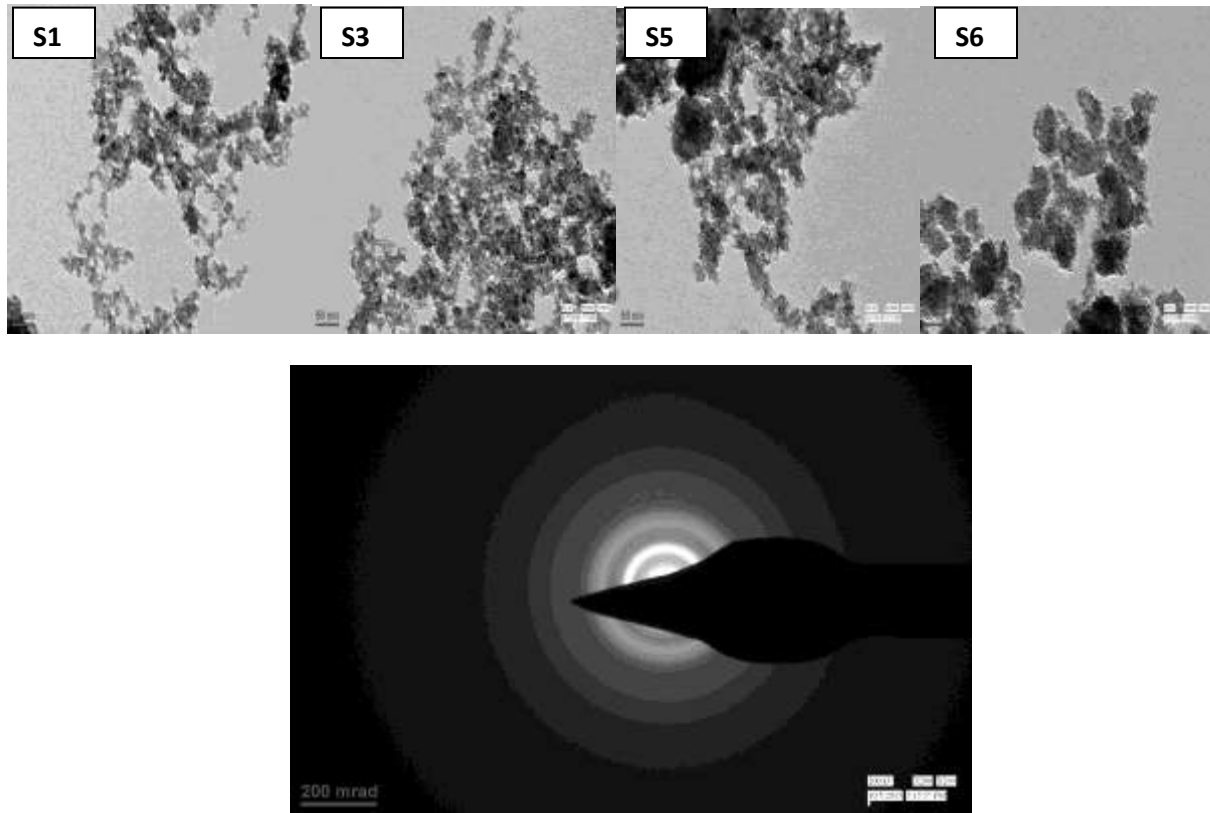


**Fig. 4:** (a)TEM micrographs of different composition of  $Cd_{1-x}Zn_xS$ : Cu, Mn ternary alloy and (b) SAED pattern of S6.

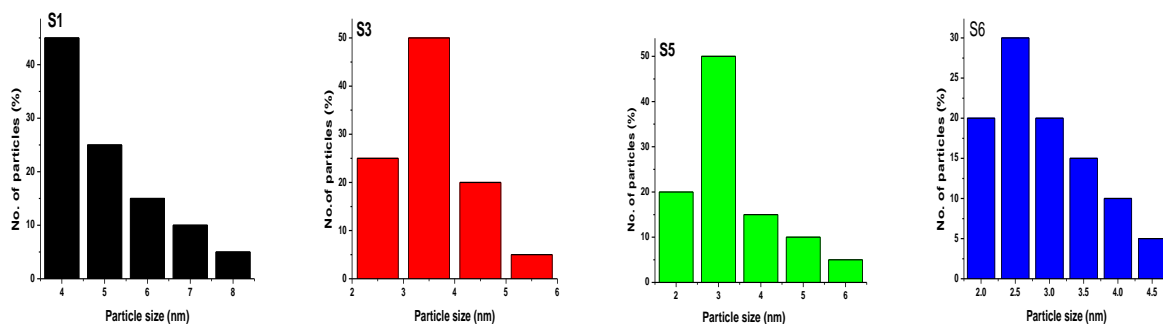


**Fig. 5:** Histograms of  $Cd_{1-x}Zn_xS$ : Cu, Mn ternary alloy at different values of mole fraction ( $x$ ).

With the increase in concentration of zinc, the crystallinity and densification is improved which is exhibited in the micrograph S5 and S6. Moreover, the agglomeration has been significantly increased. It is clear from the Fig.4 (S5 and S6) that some of the large particles are made up by agglomeration of small particles, which creates difficulty to determine the exact particle size. That's why we use the histograms for distribution of particle size as shown in the Fig. 5. The histogram represents a bar graph that illustrates frequency of occurrence versus the particle size range which was found to be ~ 2-4 nm range for the present study. There is a close agreement of particle sizes obtained by TEM and XRD analysis as given in table 2. From TEM analysis, the particle size from the micrograph of samples S1, S3, S5 and S6 is found slightly greater than as obtained by XRD results. This discrepancy may be understood due to the intrinsic defects present and dislocations in the lattice of these samples. Zhang et al<sup>23</sup> also obtained the larger crystallite size from TEM and it is possible that the obtained powder has polycrystalline nature. Therefore, it is concluded that micrographs of prepared samples show asymmetric distribution of nanoparticles due to very small nanocrystallites size. The selected area electron diffraction pattern (SAED) of sample S6 gives the diffuse diffraction rings due to small size of prepared nanocrystallites as shown in Fig 4. These rings are the confirmation of the polycrystalline nature of the prepared samples<sup>24</sup>, which also confirmed from the XRD results showing the number of diffraction peaks in different planes.

## Conclusions

Various samples of Cu, Mn codoped Cd<sub>1-x</sub>Zn<sub>x</sub>S (x= 0.0, 0.3, 0.7, 0.9) nanocrystals have been synthesized successfully by using chemical co-precipitation method. The XRD of the prepared samples with x= 0 gives wurtzite crystalline structure and exhibited the (002) plane as the preferential orientation. The average crystallite size was calculated in the range 2-4 nm corresponding to highest peak of the samples using Debye-Scherrer's formula. The presence of Cd-S/Zn-S bond, O-H and COO- groups in the samples has been confirmed by the FTIR spectroscopy. Further the TEM results confirmed agglomeration of nanoparticles in the sample.

## Acknowledgement

The authors are highly thankful to the SAIF centre, PU, Chandigarh for powder XRD measurements. The AIIMS, N. Delhi are also gratefully acknowledged for providing characterization facilities for TEM.

## References

- [1] P.K. Saini, D. Singh and D.S. Ahlawat, *Chalcogenides Lett.*, 2014, **11**, 405.
- [2] L. Andrey. Rogach, *Semiconductor Nanocrystal Quantum Dots: Synthesis, Assembly, Spectroscopy and Applications*, Springer ISBN No: 9783211752371(2008).
- [3] D. Patidar, N.S. Saxena and T. P. Sharma, *J. of Modern Optics*, 2008, **55**, 79.
- [4] P.K. Sharma, R.K. Dutta, M. Kumar, P. K. Singh and A.C. Pandey, *J. Luminescence*, 2009, **129**, 605.
- [5] A. K. Keshari and A. C. Pandey, *J. Appl. Phys.*, 2009, **10**, 5064315.
- [6] T.P. Sharma, D. Patidar, N.S. Sexena & K. Sharma, *Indian J. of Pure & Appl. Phys.*, 2006, **44**, 125.
- [7] J. H. Lee, W. C. Song, J.S. Yi, K. J. Yang, W. D. Han, J. Hwang, *Thin Solid Films*, 2003, **431**, 349.

- [8] T.Y. Lui, J.A. Zapien, H. Tang, D.D.D. Ma, Y.K. Liu, C.S. Lee, S.T. Lee, S.L. Shi and S.J. Xu, *Nanotechnology*, 2006, **17**, 5935.
- [9] J.Z. Liu, P.X. Yan, G.H. Yue, J.B. Chang, D.M. Qu, R.F. Zhuo, *J. Phys. D*, 2006, **39**, 2352.
- [10] P. Yang, M. Lu, D. Xu, D. Yuan, C. Song, *J. Phys. Chem. Solids*, 2003, **64**, 155.
- [11] K. Lui, J.Y. Jhang, X. Wu, B. Li, D. Shen, *Physica B*, 2007, **389**, 248.
- [12] G. Murugadoss, *J. Lumin*, 2012, **132**, 2043.
- [13] R. Sethi, L. Kumar, P.K. Sharma, A.C. Pandey, *Nanoscale Res. Lett*, 2010, **5**, 96.
- [14] B.D. Cullity, *Elements of X-ray diffraction*, 2<sup>nd</sup> ed. C.A. Mento Park, Addison Wesley 1978.
- [15] S. Kumar, J.K. Sharma, *Materials Science-Poland*, 2016, **34**, 368.
- [16] A. Yakoubi, T. B. Chaabane, A. Aboulaich, R. Mahiou, L. Balan, G. Medjahdi, R. Schneider, *Journal of Luminescence*, 2016, **175**, 193–202.
- [17] T.T. Nguyen, X. A. Trinh, L.H. Nguyen and T.H. Pham, *Adv. Nat. Sci: Nanosci. Nanotechnol.* 2011, **2**, 035008.
- [18] V. Narasimman, V.S. Nagarethinam, K. Usharani and A.R.Balu, *Int. J. Thin. Fil. Sci.*, 2016, **5**, 17.
- [19] I. Yadav, D.S. Ahlawat, R. Ahlawat, *Applied Physics A*, 2016, **122**, 245.
- [20] G.K. Williamson, W.H. Hall *Acta Metall*, 1951, **1**, 22-31.
- [21] M.P. Deshpande, S.H. Chaki, N.H. Patel, S.V. Bhatt, B.H. Soni, *J. Nano. Electron. Phys*, 2011, **3:1**, 193-202.
- [22] J.F.A. Oliveira, T.M. Milao, V.D. Araujo, M.L. Moreira, E. Longo, M.I.B. Bernardi, *J. Alloy. Compd.*, 2011, **509**, 6880.
- [23] Li. Zhang, D. Qin, G. Yang, Q. Zhang, *Chalcogenide Letters*, 2012, **9**, 93.
- [24] Z. Jindal, N.K. Verma, *Physica E*, 2011, **43**, 1021–1025.